# Theory of the fourfold induced-torque anisotropy in potassium

A. W. Overhauser
*Department of Physics, Purdue University, West Lafayette, Indiana 47907*

Graciela Lacueva
*Physics Department, John Carroll University, University Heights, Ohio 44118*

(Received 15 July 2002; published 30 October 2002)

Induced-torque anisotropies observed in single-crystal spheres of potassium prove that the Fermi surface is multiply connected. Cyclotron orbits which intersect heterodyne gaps created by the charge-density-wave broken symmetry lead to an anisotropic Hall effect having longitudinal components. Thereby the theoretical induced torque (in a 360° magnet rotation) has four evenly spaced minima and four maxima with a staggered spacing. The maxima grow almost $\sim H^2$ and can be 30 times higher than the minima. All such features have been observed. (Details depend on crystal growth and orientation.) All are impossible in a spherical crystal with a simply connected Fermi surface.

DOI: 10.1103/PhysRevB.66.1651XX PACS number(s): 72.15.Gd, 71.45.Lr, 71.20.−b

Potassium, the simplest metal of all, is for solid-state theory the analog of the hydrogen atom.[1] Virtually all workers, teachers, and authors believe that the conduction electrons are free-electron-like, having a Fermi surface that is essentially a perfect sphere. The experimental properties of *K* provide therefore a paradigm to test numerous aspects of the quantum theory of metals, including many-electron effects caused by Coulomb interactions.

Experimental data from diverse phenomena which severely contradict the Fermi-sphere model have accumulated during the last forty years. See Refs. 2–8 for a partial survey. These ''anomalies'' (about thirty in number) can be explained if *K* has a charge-density-wave (CDW) broken symmetry.[9] Such a broken symmetry is theoretically expected for an (otherwise bcc) alkali metal when the extreme nonlocal character of exchange and correlation[2,10] is recognized. (A CDW cannot arise in a simple metal if commonly used local-density approximations to exchange and correlation are employed.[11])

Some of the energy gaps in **k** space that arise from an incommensurate CDW having wave vector **Q** are shown in Fig. 1. **Q** is tilted slightly from the [110] direction of the reciprocal-lattice vector $\mathbf{G}_{110}$ (Ref. 12) and $Q$ is expected to be about 1.33 $(2\pi/a)$, i.e., ~6% smaller than $G_{110}$. The two families—heterodyne gaps and minigaps—are higher order gaps that arise naturally[13] when the Schrödinger equation for a conduction electron has both potentials included:

$$V(\mathbf{r}) = V_{110}\cos(\mathbf{G}\cdot\mathbf{r}) + V_Q\cos(\mathbf{Q}\cdot\mathbf{r}). \tag{1}$$

The Brillouin-zone energy gap is $V_{110}\sim 0.4$ eV and the CDW energy gap is $V_Q\sim 0.6$ eV.[8] The heterodyne gaps correspond to periodic potentials with wave vectors

$$\mathbf{G}'_n = n\mathbf{Q}', \quad \mathbf{Q}' \equiv \mathbf{G}_{110} - \mathbf{Q}, \tag{2}$$

$n=1,2,3,\ldots,$ and the minigaps have wave vectors

$$\mathbf{G}_n = (n+1)\mathbf{Q} - n\mathbf{G}_{110}, \tag{3}$$

$n=1,2,3,\ldots$. There are also second-zone minigaps, but they do not intersect the Fermi surface. The minigaps and heterodyne gaps decrease rapidly with increasing $n$. Heterodyne gaps are likely in the meV range, and minigaps are an order of magnitude larger. Unfortunately, CDW diffraction satellites have not yet been seen in *K*, so the precise **Q** is unknown.

It is clear from Fig. 1 that the Fermi surface will not only be nonspherical; it will be multiply connected (by virtue of the minigaps and heterodyne gaps). The LAK magnetotransport theorems[14] cannot then apply. Consequently the magnetoresistance need not saturate when $\omega_c\tau \gg 1$, and the high-field Hall coefficient need not be exactly $-1/nec$. ($\omega_c$

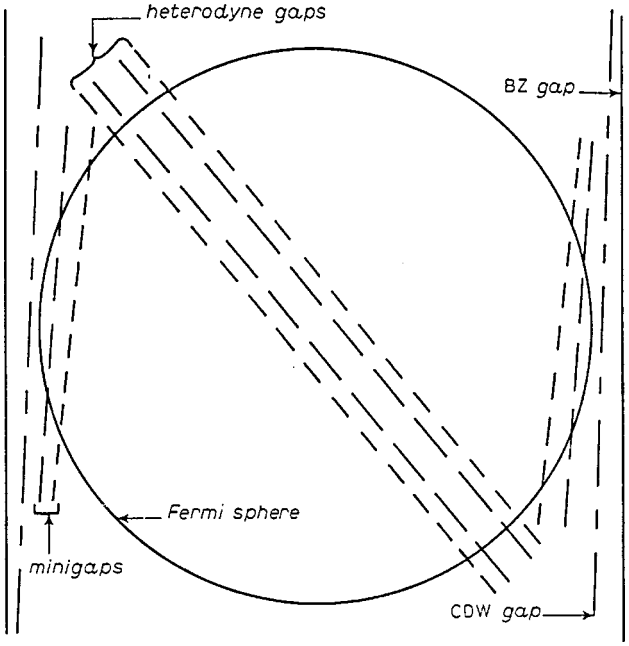


FIG. 1. Energy-gap planes in the Brillouin zone of *K* created by the combined influence of the crystal potential $V_{110}\cos(\mathbf{G}_{110}\cdot\mathbf{r})$, and the CDW potential $V_Q\cos(\mathbf{Q}\cdot\mathbf{r})$. The wave vectors associated with the heterodyne gaps and minigaps are given by Eqs. (2) and (3). The two solid lines represent faces of the Brillouin zone, and are separated by $\mathbf{G}_{110}$.

 

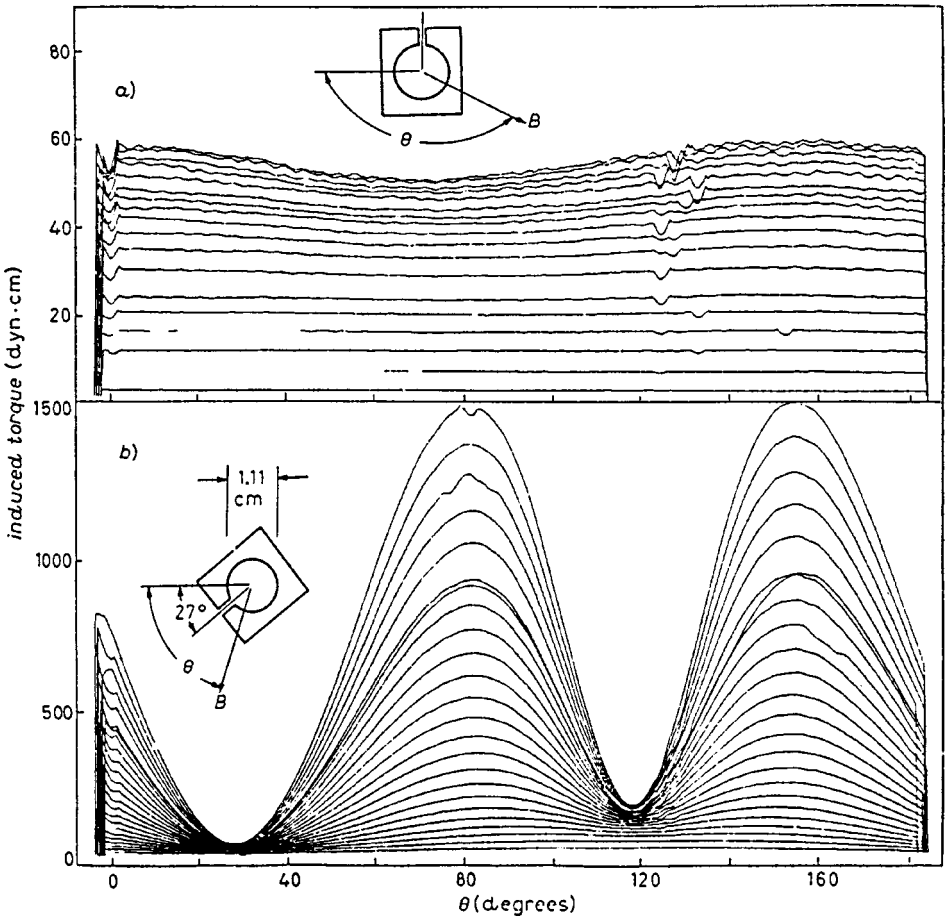


FIG. 2. Induced torque versus magnet angle $\theta$ in the horizontal plane from Ref. 17. The single-crystal sphere was grown (by the Bridgman method) in a spherical Kel-F mold, machined to a precision of 0.002 cm. The magnet rotation rate was 35°/min, i.e., $\Omega = 0.01$ rad/sec. $T = 1.5$ K. Curves are shown for $H = 1$ to 23 kG in 1 kG increments. (There are two traces for 18 kG.) In (a), the growth axis was perpendicular to the (horizontal) plane of rotation. In (b), the growth axis was in the horizontal plane.

$=eH/mc$, is the cyclotron frequency, $\tau$ the scattering time, and $n$ the electron density.) Furthermore, open orbits can occur.

The induced-torque technique is a very convenient method to study magnetoresistance since there is then no need for current or voltage leads. A spherical sample is placed in a horizontal magnetic field, which is then slowly rotated about a vertical axis. The induced currents lead to a torque $N_y$ (about this axis) which is, for a metal with an isotropic resistivity $\rho_0$ (and a simply connected Fermi surface)[15]

$$N_y = \frac{2\pi R^5 \Omega n^2 e^2 \rho_0}{15} \frac{(\omega_c \tau)^2}{1 + \left(\frac{1}{2}\omega_c \tau\right)^2}. \tag{4}$$

$R$ is the radius of the sphere and $\Omega$ the rotation rate of the magnet. The torque is isotropic, independent of the angle $\theta$ of the magnetic field **H** in the horizontal plane. $N_y$ approaches a constant value when $\omega_c \tau \gg 1$. This is the required behavior for $K$ if it has a spherical Fermi surface.

Schaefer and Marcus[16] discovered that the induced torque of single-crystal $K$ spheres is highly anisotropic. In all but seven of two hundred experiments at 4 K, on seventy different samples, $N_y(\theta)$ exhibited four large peaks in a 360° magnet rotation. The anisotropy ratios were typically 3 or 4:1 at $H = 25$ kG. The four peaks appeared irrespective of the crystallographic orientation of the spheres, even if the rotation axis was (the threefold) [111]. Indubitably, $K$ has a broken symmetry that violates its imputed cubic structure. Geometric distortion from a spherical shape was precluded by requiring torque patterns at 78 K (before further cooling to 4 K) to be accurately isotropic.

Holroyd and Datars[17] confirmed the discoveries of Schaefer and Marcus and extended them in several ways. A single-crystal sphere $(K-10)$, grown in a kel-F mold, exhibits a 30:1 anisotropic torque $(H = 23\,\text{kG})$ when the growth axis is in the horizontal plane, as shown in Fig. 2. Another sphere $(K-4)$, grown in oil (but with the oil removed) had an isotropic torque. However, an identical sample $(K-2)$ with surface oil had a 6:1 anisotropic torque $(H = 22\,\text{kG})$.

The extraordinary variations described above are easy to understand. The optical anisotropy of $K$ requires that there is only a single **Q** for each domain.[18] There are, of course, 24 equivalent axes that **Q** might have. If they are equally represented in a macroscopic sphere, the torque pattern $(H \leqslant 23\,\text{kG})$ should be isotropic. However, elastic stress created by cooling (below the freezing point of oil) can lead to an orientational **Q**-domain texture and, consequently, to the fourfold torque anisotropy, as we show below.

At higher fields, $40 < H \leqslant 85$ kG, 20–30 sharp, open-orbit resonances appear in the induced-torque patterns.[3] This truly spectacular phenomenon, observed in all eighteen $K$ samples studied, has been explained,[5] based on the multiply connected Fermi surface of Fig. 1.

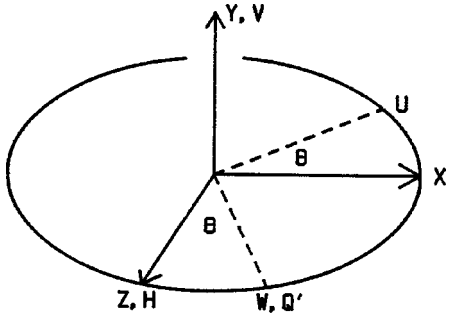


FIG. 3. Coordinate systems employed to describe the resistivity tensor $\rho_{xyz}$ or $\rho_{uvw}$. The heterodyne-gap wave vector $\mathbf{Q}'$ is taken to be in the $\hat{x}\hat{z}$ plane, at an angle $\theta$ from the magnetic field $\mathbf{H}$. (A positive increment in $\theta$ here, and in Fig. 6, corresponds to a negative increment in Fig. 2.)

The purpose of the present work is to derive the torque pattern shown in Fig. 2. Suppose $K$ has a spherical Fermi surface. Then, with $\mathbf{H}$ along the $\hat{z}$ axis, the resistivity tensor in the $\hat{x}\hat{y}\hat{z}$ frame is

$$\rho_{xyz}=\rho_0\begin{pmatrix} 1 & \omega_c\tau & 0 \\ -\omega_c\tau & 1 & 0 \\ 0 & 0 & 1 \end{pmatrix}. \tag{5}$$

We shall examine the effect of one pair of heterodyne gaps and assume that $\mathbf{Q}'$ lies in the $\hat{x}\hat{z}$ plane, an angle $\theta$ from $\mathbf{H}$ and parallel to $\hat{w}$, as shown in Fig. 3. The resistivity tensor in the $\hat{u}\hat{v}\hat{w}$ frame is

$$\rho_{uvw}=S^{-1}\rho_{xyz}S, \tag{6}$$

where

$$S=\begin{pmatrix} \cos\theta & 0 & \sin\theta \\ 0 & 1 & 0 \\ -\sin\theta & 0 & \cos\theta \end{pmatrix}. \tag{7}$$

$S^{-1}$ is the transpose of $S$. Accordingly,

$$\rho_{uvw}=\rho_0\begin{pmatrix} 1 & \omega_c\tau\cos\theta & 0 \\ -\omega_c\tau\cos\theta & 1 & -\omega_c\tau\sin\theta \\ 0 & \omega_c\tau\sin\theta & 1 \end{pmatrix}. \tag{8}$$

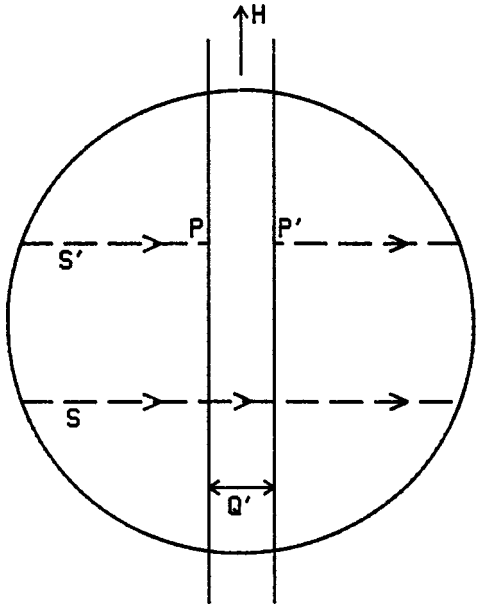


FIG. 4. Cyclotron orbits $S$ and $S'$ on the Fermi surface (in $\mathbf{k}$ space). The heterodyne-gap planes are the two vertical lines. If the heterodyne gap $E_g$ is very small, the orbit $S$ will "pass through" the energy gaps, i.e., magnetic breakdown. If $E_g$ is sufficiently large, the electron on orbit $S'$ will proceed instantly from $P$ to $P'$ (because they are in fact the same quantum state).

Consider Fig. 4 and the two (vertical) heterodyne-gap planes. A magnetic field $H\cos\theta$ parallel to $\mathbf{Q}'$ would support ordinary cyclotron orbits, unaffected by the heterodyne gaps. Consequently the $uv$ and $vu$ elements of the tensor (8) remain unchanged. However, for a magnetic field, $H\sin\theta$, parallel to a vertical line in Fig. 4, a typical cyclotron orbit $S$ would obtain if the heterodyne gap is $E_g=0$. If $E_g\neq 0$, then on orbit $S'$ (in Fig. 4) the points $P$ and $P'$ have the same wavefunction. So the time it would ordinarily take to travel from $P$ to $P'$ is not required. This effect corresponds to a Bragg-like reflection in real space; but in momentum space, to an instantaneous "Bragg advance." Consequently the effective cyclotron frequency for the $vw$ and $wv$ elements of the tensor (8) must be increased from $\omega_c$ to $\omega_c(1+\gamma)$:

$$\rho_{uvw}=\rho_0\begin{pmatrix} 1 & \omega_c\tau\cos\theta & 0 \\ -\omega_c\tau\cos\theta & 1 & -\omega_c\tau(1+\gamma)\sin\theta \\ 0 & \omega_c\tau(1+\gamma)\sin\theta & 1 \end{pmatrix}. \tag{9}$$

One can show that, $\gamma\approx 3Q'/4k_F$, for the simple case just considered. (We will modify $\gamma$ below to treat magnetic breakdown effects and additional heterodyne gaps.)

The corrected resistivity tensor in the $\hat{x}\hat{y}\hat{z}$ frame is obtained by the inverse transformation

$$\rho_{xyz}=S\rho_{uvw}S^{-1}. \tag{10}$$

Accordingly, from Eqs. (7) and (9)

$$\rho_{xyz}=\rho_0\begin{pmatrix} 1 & \omega_c\tau(1+\gamma\sin^2\theta) & 0 \\ -\omega_c\tau(1+\gamma\sin^2\theta) & 1 & -\omega_c\tau\gamma\sin\theta\cos\theta \\ 0 & \omega_c\tau\gamma\sin\theta\cos\theta & 1 \end{pmatrix}. \tag{11}$$

The *xy* and *yx* components require the Hall coefficient to be larger in magnitude than, $1/nec$ (the rigorous prediction for a simply connected Fermi surface). Significant Hall enhancements $\sim 4-8\,\%$, depending on single-crystal orientation, have been observed (by helicon resonances at high fields) in both slab[19] and spherical[20] geometries.

The most remarkable feature of the tensor (11) is the appearance of *yz* and *zy* components. These can be described as a ''longitudinal Hall effect,'' i.e., a current in the $\hat{y}$ direction creates an electric field parallel to **H**. The existence of this longitudinal Hall effect was postulated and shown to cause a four-peaked, induced-torque anisotropy,[21] but a derivation (as given above) was unknown.

Of course, the torque $N_y$ is no longer given by Eq. (4). Visscher and Falicov[22] have derived an expression for $N_y$, applicable to a general resistivity tensor

$$N_y=\frac{4\pi R^5\Omega B^2}{15c^2}\,\frac{\lambda}{\lambda(\rho_{yy}+\rho_{zz})-\mu}, \tag{12}$$

where

$$\lambda=(\rho_{xx}+\rho_{zz})(\rho_{xx}+\rho_{yy})-\rho_{yz}\rho_{zy} \tag{13}$$

and

$$\mu=(\rho_{xx}+\rho_{zz})\rho_{xz}\rho_{zx}+(\rho_{xx}+\rho_{yy})\rho_{xy}\rho_{yx}+\rho_{xy}\rho_{yz}\rho_{zx}+\rho_{xz}\rho_{zy}\rho_{yx}\,. \tag{14}$$

For the tensor (11) there is considerable simplification:

$$N_y=\frac{2\pi R^5\Omega n^2e^2\rho_0}{15}\,\frac{(\omega_c\tau)^2[4+(\omega_c\tau\gamma\sin\theta\cos\theta)^2]}{4+(\omega_c\tau\gamma\sin\theta\cos\theta)^2+[\omega_c\tau(1+\gamma\sin^2\theta)]^2}, \tag{15}$$

which reduces to Eq. (4) if $\gamma=0$. It is clear from the $\theta$ dependence that a four-peaked anisotropy occurs for $\omega_c\tau\gg 1$, and that the torque peaks grow roughly as $H^2$ in the high-field limit.

In order to fit Eq. (15) to the data of Fig. 2 it is necessary to introduce magnetic breakdown of the heterodyne gaps. If an energy gap $E_g$ is small and if an electron is approaching (in momentum space) rapidly, there is a probability $P_B$ that the electron will not be ''Bragg advanced'' at the energy gap. Instead, it will continue on its initial orbit in *k* space as if the energy gap were not there. An invariant expression for $P_B$ based on original examples[23,24] is[25]

$$P_B=\exp\left[\frac{-\pi mcE_g^2}{2\hbar^2e|\mathbf{v}\cdot(\mathbf{K}\times\mathbf{H})|}\right], \tag{16}$$

where **K** is the wave vector of the periodic potential producing the energy gap $E_g$ and **v** is the velocity that the electron would have at the gap if it were free. For the present purpose the breakdown probability reduces to

$$P_B=\exp\left[\frac{-H_0}{H|\sin\theta|}\right], \tag{17}$$

where $\theta$ is, as in Fig. 3, the angle between $\mathbf{Q}'$ and **H**. The appearance of $|\sin\theta|$ in the denominator, was first emphasized by Reitz.[25] $H_0$ combines all the other factors in Eq. (16) and is frequently called the breakdown field; it will be

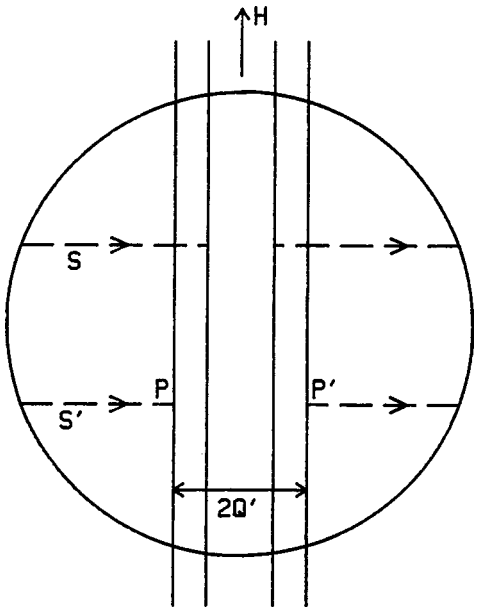


FIG. 5. Cyclotron orbits *S* and $S'$ on the Fermi surface, intersected by two pairs of heterodyne gaps. The orbit *S* is broken down at the outer pair, but is ''Bragg advanced'' by the inner pair. The orbit $S'$ advances from *P* to $P'$ if the outer pair is not broken down.

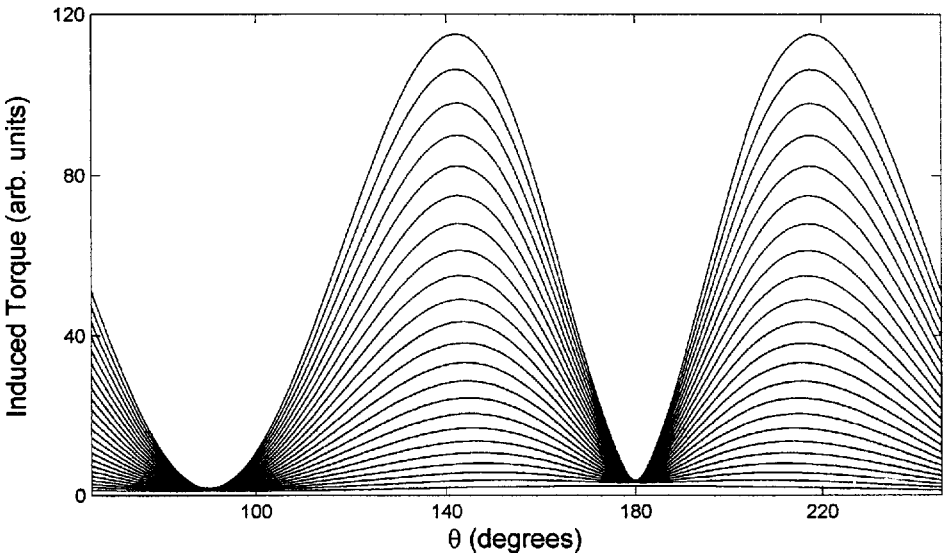


FIG. 6. Theoretical induced-torque anisotropy based on the resistivity tensor (11), calculated from Eq. (15) and incorporating the breakdown phenomenon modeled by Eq. (18), in accordance with Fig. 5. The torque peaks have staggered separations 75°, 105°, 75°, 105°, in agreement with the data of Fig. 2. The parameters used in Eqs. (15) and (18): $\gamma_0 = 0.4$, $H_0 = 2.12$ kG, $\omega_c\tau = 2.5$ H, with $H$ in kG.

an adjustable parameter.

Since the heterodyne gaps decrease rapidly with $n$, in Eq. (2), and since $H_0$ is proportional to $E_g^2$, we will take (as an approximate model) the two-channel option depicted in Fig. 5. We assume that all heterodyne gaps for $n>2$ are always broken down, and that the heterodyne gap for $n=1$ is sufficiently large to not break down when $H \leqslant 23$ kG. Accordingly, orbit $S'$ in Fig. 5 will occur with probability $1-P_B$, so the remaining channel $S$ will be assigned probability $P_B$. The value of $\gamma(H)$, which appears in Eqs. (9), (11), and (15) will then be

$$\gamma(H) = \gamma_0 \left[ 2 - \exp\left( \frac{-H_0}{H|\sin\theta|} \right) \right]. \tag{18}$$

Figure 6 illustrates the fit of Eqs. (15) and (18) to the data of Fig. 2. (The data for $180° \leqslant \theta \leqslant 360°$ are identical to $0 \leqslant \theta \leqslant 180°$.) The torque minima are evenly spaced: 90°, 90°, 90°, 90°. However, the torque maxima are staggered: 75°, 105°, 75°, 105°, as observed. The peak height vs $H$ for $\theta = 155°$ in Fig. 2 is shown in Fig. 7 along with the (fitted) theoretical curve. The dashed line ($\sim H^2$) indicates that the theoretical torque maxima deviate slightly from an $H^2$ dependence.

It is known from low-field ($H < 3$ kG) induced torque data[3,16,26] that the residual resistivity $\rho_0$ is very anisotropic. This feature is caused by impurity-induced, CDW-umklapp scattering.[27] For simplicity we have ignored this feature, which has an interesting field dependence,[28] in order that the

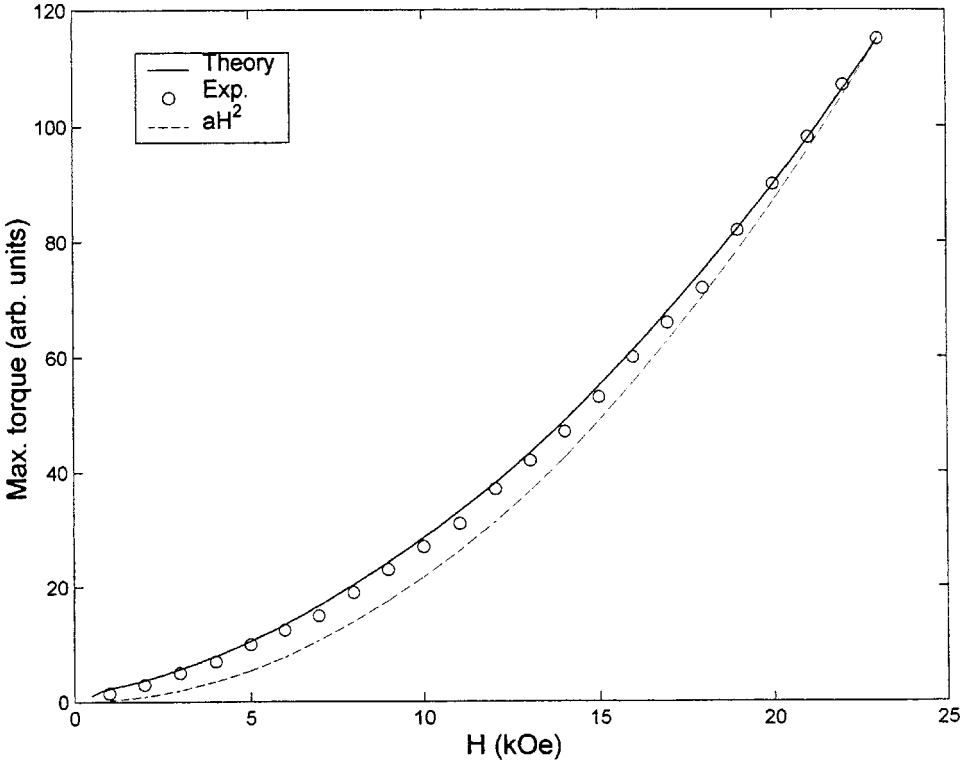


FIG. 7. Magnetic field dependence of the torque peaks (at $\theta = 155°$ in Fig. 2). The solid curve is the theoretical behavior from Fig. 6. The dashed curve is a pure $H^2$ behavior, shown only to provide a comparison with the theoretical shape.

behavior of Eq. (15) can be intelligible and uncomplicated. The comparative data near the torque minima of Figs. 2 and 6 indicate the relevance of an anisotropic residual resistivity.

The extraordinary anisotropy of sample K-10, shown in Fig. 2, requires a highly oriented **Q**-domain texture. The theoretical treatment given above was tractable because we considered only a single **Q** domain and, even then, neglected many of the gaps shown in Fig. 1. Very likely the growth axis of K-10 was [110]. In such a case, a **Q**-domain texture for which the [110] direction would be prominent in the data could comprise four **Q** domains (in approximately equal volumes) with hypothetical **Q**'s:

$$(1.0,0.9,0.1),(1.0,0.9,-0.1),(0.9,1.0,0.1),(0.9,1.0,-0.1), \tag{19}$$

(together with minor populations from the twenty other **Q** domains). Since most *K* single-crystal spheres have a torque anisotropy of 3 or 4:1, their **Q**-domain textures must be more nearly random (compared to K-10) but with a preferred bias created by elastic stress or other metallurgical history.

The anomalous terms, proportional to $\gamma$, in Eq. (11) can also be derived by computing the conductivity tensor $\sigma$ with the help of the Chambers path-integral method,[29] and then inverting $\sigma$ to obtain $\rho$. (This calculation is extremely tedious.) One does indeed reproduce the anomalous Hall terms of Eq. (11). Terms which create an open-orbit resonance also appear. We disregard them here because they are unimportant for $H<30$ kG. They are treated in full elsewhere.[5]

In conclusion the induced-torque anisotropy of single-crystal *K* spheres shows that *K* does not have a simply connected Fermi surface. The data requires an anisotropic Hall effect, indeed one with longitudinal components. Heterodyne gaps, which are a natural consequence of a CDW broken symmetry, explain the four-peaked patterns, including the staggered angular intervals between maxima as well as their field dependence. They also explain the anomalous Hall coefficients observed with helicons.


[1] *K* remains bcc on cooling to 4 K, unlike Li and Na, which transform to a rhombohedral 9*R* phase: A. W. Overhauser, Phys. Rev. Lett. **53**, 64 (1984).

[2] A. W. Overhauser, in *Highlights of Condensed-Matter Theory, Proceedings of the International School of Physics "Enrico Fermi," Course LXXXIX, Varenna on Lake Como*, 1983, edited by F. Bassani, F. Fumi, and M. P. Tosi (North-Holland, Amsterdam, 1985), p. 194.

[3] P. G. Coulter and W. R. Datars, Can. J. Phys. **63**, 159 (1984).

[4] G. L. Dunifer, J. F. Sambles, and D. A. H. Mace, J. Phys.: Condens. Matter **1**, 875 (1989).

[5] M. Huberman and A. W. Overhauser, Phys. Rev. B **25**, 2211 (1982).

[6] Graciela Lacueva and A. W. Overhauser, Phys. Rev. B **46**, 1273 (1992).

[7] Mi-Ae Park and A. W. Overhauser, Phys. Rev. B **55**, 1398 (1997).

[8] A. W. Overhauser, Adv. Phys. **27**, 343 (1978).

[9] A. W. Overhauser, Phys. Rev. **167**, 691 (1968).

[10] A. W. Overhauser, Phys. Rev. B **2**, 874 (1970).

[11] A. W. Overhauser, in *Electron Correlations in Solids, Molecules and Atoms*, edited by Jozef T. Devreese and Fons Brosens (Plenum, New York, 1983), p. 41.

[12] G. F. Giuliani and A. W. Overhauser, Phys. Rev. B **20**, 1328 (1979).

[13] F. E. Fragachán and A. W. Overhauser, Phys. Rev. B **29**, 2912 (1984).

[14] I. M. Lifshitz, M. Ia Azbel, and M. I. Kaganov, Zh. Eksp. Teor. Fiz. **31**, 63 (1956) [Sov. Phys. JETP **4**, 41 (1957)]; see also: E. Fawcett, Adv. Phys. **13**, 139 (1964).

[15] J. S. Lass and A. B. Pippard, J. Phys. E **3**, 137 (1970).

[16] J. A. Schaefer and J. A. Marcus, Phys. Rev. Lett. **27**, 935 (1971).

[17] F. W. Holroyd and W. R. Datars, Can. J. Phys. **53**, 2517 (1975).

[18] A. W. Overhauser and N. R. Butler, Phys. Rev. B **14**, 3371 (1976).

[19] D. E. Chimenti and B. W. Maxfield, Phys. Rev. B **7**, 3501 (1973).

[20] S. A. Werner, T. K. Hunt, and G. W. Ford, Solid State Commun. **14**, 1217 (1974).

[21] Xiaodong Zhu and A. W. Overhauser, Phys. Rev. B **30**, 622 (1984).

[22] P. B. Visscher and L. M. Falicov, Phys. Rev. B **2**, 1518 (1970).

[23] E. I. Blount, Phys. Rev. **126**, 1636 (1962).

[24] John R. Reitz, J. Phys. Chem. Solids **25**, 53 (1964).

[25] Ref. 5, Eq. (16).

[26] M. Elliott and W. R. Datars, J. Phys. F: Met. Phys. **13**, 1483 (1983).

[27] Marilyn F. Bishop and A. W. Overhauser, Phys. Rev. B **18**, 2447 (1978).

[28] M. Huberman and A. W. Overhauser, Phys. Rev. B **31**, 735 (1985).

[29] R. G. Chambers, Proc. R. Soc. London, Ser. A **202**, 378 (1950).